American Mineralogist, Volume 91, pages 1857–1862, 2006

Recovery of stishovite-structure at ambient conditions out of shock-generated amorphous silica

OLIVER TSCHAUNER,[1,3,*] SHENG-NIAN LUO,[2] PAUL D. ASIMOW,[3] AND THOMAS J. AHRENS[4]

[1]High Pressure Science and Engineering Center and Department of Physics, University of Nevada, Las Vegas, Nevada 89154, U.S.A.
[2]P-24 Plasma Physics, Los Alamos National Laboratory, Los Alamos, New Mexico 87545, U.S.A.
[3]Division of Geological and Planetary Sciences, California Institute of Technology, Pasadena, California 91125, U.S.A.
[4]Lindhurst Laboratory of Experimental Geophysics, Seismological Laboratory, California Institute of Technology, Pasadena, California 91125, U.S.A.

ABSTRACT

We show that bulk amorphous silica recovered from shock-wave experiments on quartz to 57 GPa is not a true glass but rather keeps a large degree of long-range structural information that can be recovered by static cold recompression to 13 GPa. At this pressure, shock-retrieved silica assumes the structure of crystalline stishovite. A minor amount of material recovers the structure of a recently discovered new silica polymorph.

Keywords: Meteorite, shock, phase transition, amorphous to solid, XRD data, stishovite, high pressure

INTRODUCTION

The observation of the high-pressure silica phases coesite and stishovite in terrestrial impact craters like Canyon Diablo (Chao and Shoemaker 1960) and Nördlinger Ries (Shoemaker and Chao 1961) is generally taken as evidence for shock-induced, high-pressure conditions during impacts of large meteorites on Earth. Similarly, these phases are found in meteorites that record a history of impact events in the early solar system (e.g., Stöffler et al. 1991). More recently, so-called post-stishovite phases of the scrutinyite (i.e., α-PbO_2) and baddeleyite type have been found in melt pockets in the Martian meteorite Shergotty (Sharp et al. 1999; El Goresy et al. 2000; Dera et al. 2002). These phases become stable above a static pressure of 100 GPa (Ono et al. 2002; Murakami et al. 2003). It has been extremely challenging to verify the interpretation of impact-induced formation of these phases using laboratory shock experiments, as silica retrieved from shock experiments to pressure-temperature conditions within the stability field of these high-pressure phases is usually amorphous (Wackerle 1962; DeCarli and Milton 1965; Kleeman and Ahrens 1973; Luo et al. 2004). The consistency between the calculated and observed pressure-volume-temperature relations along the Hugoniot of silica exposed to single shock supports the suggestion that quartz and fused silica transform to stishovite during laboratory shock experiments, yet only amorphous material is retrieved from experiments along the principal Hugoniot (Luo et al. 2003). Experimental data from shock release from the principal Hugoniot strongly indicate back transformation of dense silica to material having densities between 3.0 and 2.1 g/cm^3 (compared to the density of vitreous silica of 2.2 g/cm^3) (Luo et al. 2003).

Thus, traces of stishovite reported from shock experiments (DeCarli and Milton 1965; Kleeman and Ahrens 1973) may represent locally different shock conditions, as from shear-heating of otherwise amorphous dense silica during shock (Grady 1980; Tan and Ahrens 1990). Residual heat deposited during irreversible shock compression is liberated as excess temperature along the quasi-isentropic release path from high-pressure states generated by single shocks. Common wisdom is that the resulting high temperature (Wackerle 1962; Boslough 1988) induces back transformation of stishovite toward lower density states and subsequent vitrification, i.e., formation of a material with only medium-range order. The alternative is structural release of dense amorphous silica that never assumed the stishovite structure (Gratz et al. 1992; Sharma and Sikka 1996; Fiske et al. 1998). Despite these ambiguities concerning the shock transformation history of silica, characteristic deformation features in quartz and the amorphous state are commonly used to estimate the peak pressure of rocks subjected to natural impacts (Chao 1967; Stöffler 1971; Kieffer et al. 1976; Langenhorst et al. 1992; Luo et al. 2003).

Here we report findings which show that shock-retrieved amorphous silica actually maintains a large degree of long-range structural information and that this material transforms into crystalline stishovite and a recently discovered metastable high-pressure polymorph (Luo et al. 2004) upon rather gentle processing, by cold compression to 13 GPa. We argue that this demonstrates memory of the structures present in the shock state, and therefore strongly supports the inference of formation of stishovite or a closely related crystalline phase on the Hugoniot. Furthermore, it suggests a method for reversing the effects of amorphization upon release of shock products in general, and hence a way to extract additional information on shock conditions in meteorites and impact crater materials.

EXPERIMENTAL METHODS

History of the sample

We used amorphous dense silica retrieved from the shock experiment S1168, which has been described in detail elsewhere (Luo et al. 2004; Tschauner et al. 2004). In that experiment, a doubly polished disk of single-crystal quartz oriented along the (0001) direction was encased in a recovery chamber made from 304-stainless steel. The sample was shocked to peak conditions of 57 GPa and 2100 K by reverberation of shocks within the steel sample chamber because the impedance contrast between steel and silica allow for multiple reflections of the shock wave in the silica sample, thus achieving the shock pressure of the steel asymptotically

* E-mail: olivert@physics.unlv.edu

while the sequence of shock states up to the peak pressure is close to states on an isentrope (Luo et al. 2003). The initial shock temperature was obtained along the principal Hugoniot. Subsequent further compression and heating by reverberation assumed an isentrope following the procedure of Luo et al. (2003). After recovery, the sample was characterized by Raman spectroscopy and by powder X-ray diffraction, and found to be amorphous except for a few vol% of Fe-metal and of a new silica phase intermediate between fourfold- and sixfold-coordinated silica, which had been characterized and described already from diamond-anvil cell experiments on tridymite (Luo et al. 2004). It is interesting that there is a small amount of Fe-metal in the sample, despite its optical clarity. Metal spherules of sub-micrometer diameter have been often found in materials shocked in steel sample chambers (Stöffler et al. 1991; Langenhorst et al. 2002). They probably result from local melting of iron at small gaps along the border between sample and steel chamber and are injected even into solid sample material by the large particle velocity of iron during shock and upon release (Tschauner et al. 2005).

Six months after recovery, no Bragg scattering of any crystalline silica phase could be detected. Thus the new silica phase became amorphous over the turn of half a year consistent with its intermediate structural character. A clear, homogeneous piece of sample, 50 µm in diameter, was separated from this X-ray amorphous material and characterized by Raman spectroscopy. However, the Raman spectrum did not exhibit any structural features. Although intense broadband fluorescence from defects limits accumulation time and makes background correction difficult, this apparent absence of a Raman signal indicates that, in our sample, vibrational coherence length is markedly smaller than 500 nm, the excitation wavelength of the probe laser. Under crossed polarizers, the sample exhibited optical anisotropy, which could be from residual stress in a genuinely structureless material, or could be an intrinsic property of the material due to structure not visible with X-ray or Raman techniques. As we reported previously (Tschauner et al. 2004), we loaded this specimen into a diamond cell using Ar as a pressure medium and collected diffraction patterns upon compression allowing for a 5 min interval between each pressure increase. We observed an amorphous-to-solid transition at 13 GPa, 300 K. At the preceding pressure of 10 GPa, there was no indication of crystallization. The transition occurred within less than this increment of 3 GPa and over less than 300 s. Based on the fact that the reflections were those of a single crystal with large mosaic spread rather than a powder, we concluded that the amorphous-to-crystal transition was not a seed-triggered mechanism. However, the nature of the crystalline phase remained unclear.

Present experiment

We released pressure from the point of onset of crystallization to ~3 GPa within 10 min and recovered the sample after keeping it at this pressure for 5 hours. Immediately after retrieval from the diamond cell, we collected a sequence of diffraction patterns at ambient pressure at the 16ID-B undulator beamline at the High-Pressure Collaborative Access Team (HPCAT), section 16 of the APS-ANL synchrotron, using a monochromatic beam of wavelength 0.3699 Å (33.52 ± 0.05 keV) and a Mar345 image plate detector. The accumulation time for each pattern was 500 s. During accumulation the sample was oscillated along ω by ±15°, hence along an axis perpendicular to the X-ray primary beam vector, while all other angular positions were kept fixed.

Over the course of accumulations, the diffraction signal manifested increasing crystallinity. Also, the initial single-crystal-like order that we observed in situ at 13 GPa evolved into a pattern exhibiting several sharp Bragg reflections, consistent with an assembly of a few crystallites with diameters on the order of 10 µm (Fig. 1). The size of these crystallites was estimated from comparative runs on similar coarse-grained assemblies using the same X-ray focal spot size at the same beamline. Furthermore, as the pattern evolved, we noted development of faint, smooth Debye-fringes at different 2θ angles (Fig. 1). This evolution can be the result of irradiation or of stress-relaxation in the retrieved sample. As we discuss below, irradiation has no influence on the crystalline state of the sample, however.

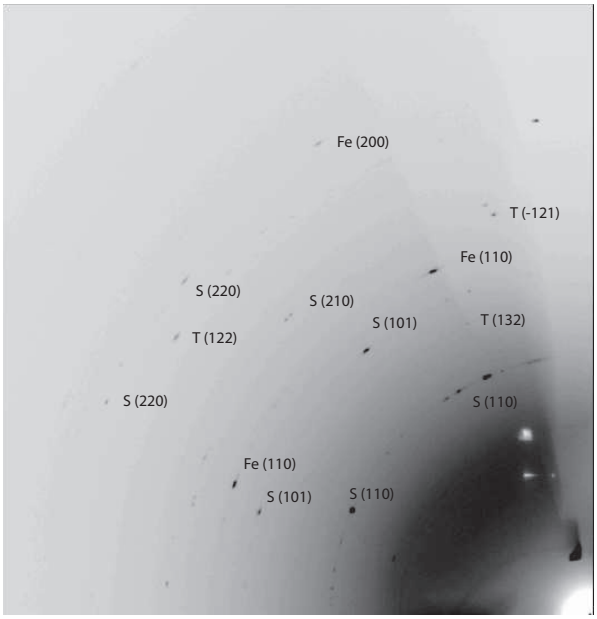

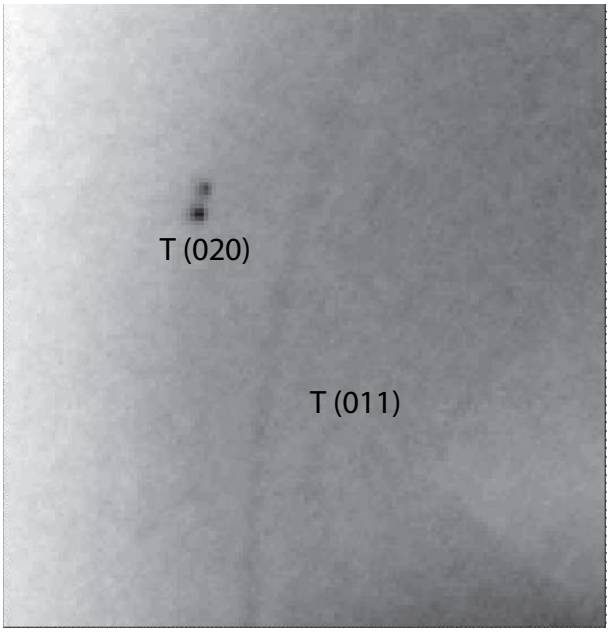

FIGURE 1. Diffraction pattern of the sample after third exposure. The pattern consists mostly of a few slightly elongated spots from Bragg diffraction of a small number of crystallites having different orientations. The elongation results from the oscillation of the sample along ω during accumulation, and indicates a large halfwidth of these single-crystal reflections which is typical for defect-rich solids. Rather smooth Debye-fringes occur at low angles and belong to the (011) and (020) reflections of the transitory silica phase (Luo et al. 2004; Tschauner et al. 2005). In the image, these fringes are obscured by the pronounced diffuse elastic and Compton scattering from the sample centered around 0° 2θ. Miller indices labeled with "S" and "T" belong to stishovite and the transitory silica phase, respectively, while reflections from Fe-metal are labeled "Fe." Insert: The (020) and (011) reflections of the transitory phase. Most diffractions from this phase form individual peaks with a marked mosaic spread. However, the (011) diffraction is a smooth Debye ring, indicating that the transitory phase has much finer granularity, at least in part, than coexisiting stishovite.

RESULTS

The observed diffraction pattern originates from several crystallites of different size and orientation and they occur along with powder-diffraction features. Consequently, we integrated the pattern along the azimuthal angle after correction for geometric distortions (Hammersley et al. 1996) to index the observed diffraction peaks based on 2θ angles only.

The peaks from the two lowermost, smooth diffraction fringes (see caption of Fig. 1) match the two most pronounced peaks of the recently documented metastable high-pressure silica polymorph intermediate between fourfold and sixfold coordination (Luo et al. 2004; Tschauner et al. 2004). Subsequently, 34 diffraction features in the integrated pattern were identified as belonging to this phase (Fig. 2, upper panel, and Table 1). Four other peaks belong to Fe metal, and 11 remaining peaks were indexed unambiguously as stishovite (Fig. 2, lower panel, and Table 1). We optimized the cell parameters of all three phases using the Jade 7.5+ software package. The diffraction pattern is dominated by stishovite (Fig. 2, lower panel) with about 10 to 25% of the recently documented metastable high-pressure silica polymorph intermediate between fourfold and sixfold coordination (Luo et al. 2004) shown in the upper panel of Figure 2. Most of the single-crystal Bragg reflections belong to stishovite whereas the transitory silica polymorph exhibits diffraction features partially arranging to fringes (Fig. 1, inset), partially remaining as individual spots. We note that observed and calculated intensities in Figure 2 show only a rough match, as most of the observed diffraction intensity is averaged over just a few differently oriented crystallites and do not represent the statistical average of a powder diffraction pattern.

The spotty pattern of stishovite makes a more precise quantification of the relative fractions of phases impossible and precludes any weighting of structure factors during refinement. The optimized cell parameters and a list of calculated and observed *d*-spacings of the symmetry-allowed reflections for both phases are given in Table 1. The cell volume of stishovite in our experiment (49.71 Å^3) is 7 to 8.8% larger than pristine stishovite at ambient conditions (Kirfel et al. 2001). This finding is not a surprise, since the present stishovite sample is the result of a structural recovery process upon cold compression of amorphous material. The enlarged volume indicates a high defect density

TABLE 1. Observed and calculated reflections of stishovit and the new transitory silica phase

Observed Bragg reflections	Assignment			
d_{obs} (Å)	d_{calc} (Å) stishovite	(*hkl*) stishovite	d_{calc} (Å) transitory phase	(*hkl*) trans. phase
–			7.497	010
4.150			4.153	011
3.742			3.749	020
3.036	3.045	110		
–			2.997	021
2.495			2.499 + 2.494	030 + 002
2.380			2.367	012
2.239			2.234	031
2.284	2.276	101		
2.224			2.223	101
–	2.153	200		
2.132			2.131	111
2.078			2.077	022
2.017	2.012	111		
1.928	1.926	210		
1.913			1.912	121
1.876			1.874	040
–			1.765	032
1.753			1.754	041
1.711			1.713	112
1.625			1.623	131
1.587			1.593	122
–	1.564	211		
1.524	1.523	220		
1.518			1.520	023
1.508			1.499 + 1.498	050 + 042
1.440			1.439 + 1.436	132 + 051
–			1.433	141
1.384			1.384 + 1.382	033 + 103
1.357	1.362	310	1.359	113
1.338	1.340	002		
1.328	1.324	221		
1.296			1.296	123
1.284			1.285	052
1.282			1.283	142
1.256			1.250	060
1.248			1.247	004
1.241			1.244 + 1.243 + 1.241	043 + 151 + 200
1.235			1.230	014
1.045	1.045	410		

Notes: The cell parameters of the latter are $a = 2.482 \pm 0.003$, $b = 7.497 \pm 0.008$, $c = 4.988 \pm 0.003$ Å, the volume is 92.86 Å^3, which is the same as reported previously (Luo et al. 2004). The cell parameters for stishovite are $a = 4.307 \pm 0.006$, $c = 2.680 \pm 0.006$ Å, and the volume is 49.71 Å^3, which is quite large for stishovite and indicates lack of structural order as upon vitrification, or in the present case upon recovery from amorphous material. Further noticeable Bragg peaks at 2.094, 1.472, 1.045, and 0.934 Å in the pattern shown in Figure 2 are the reflections (110), (200), (220), (310) from α-Fe.

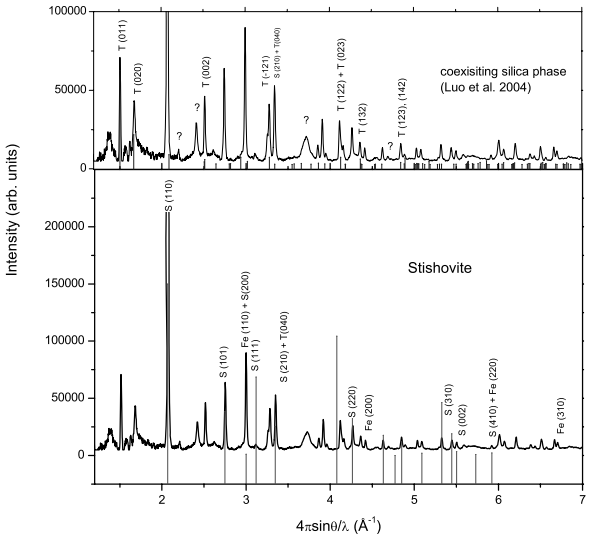

FIGURE 2. Diffraction pattern after integration and background subtraction. The background was fitted with a spline using 10 fixed points using the Jade 7.5 package. The pattern from the experiment is compared to the calculated and integrated diffraction pattern of stishovite (red bars in the lower panel) and the transitory silica phase (blue bars in the top panel). Some of the observed higher- and middle-angle reflections are labeled. Observed and calculated intensities show only a rough match, because the observed diffraction intensity is averaged over just a few differently oriented crystallites and do not represent the statistical average of a powder diffraction pattern. Question marks indicate peaks that do not belong to stishovite, the transitory phase, or Fe metal; however, they may belong to a few percent of Fe_2N-type silica. Furthermore, there is a broad, "glassy" peak below 1.5 Å^{-1}, which may belong to disordered material of the transitory silica phase and Fe_2N-type silica.

similar to that found upon onset of bulk vitrification of stishovite (Luo et al. 2006) and other materials at ambient pressure and during transition of radioactive solids into metamict state (Ewing 1999). It is more surprising that this enlarged volume does not go along with a reduction of crystal symmetry: we did not find any indication for reduced symmetry in the collected patterns such as peak splitting and occurrence of new reflections at Q-vectors symmetry-forbidden for the space group of stishovite, $P4_2/mnm$.

Four unidentified peaks labeled by question marks in Figure 2 can be assigned to Fe_2N-like silica (Liu et al. 1978; Sekine et al. 1987) as a minor phase comprising a few percent of the sample. In this case, several other observed peaks may be overlaps of reflections from this phase and the transitory silica phase. For this phase, we fit a cell with dimensions $8.48 \times 4.21 \times 5.19$ Å^3 and $\beta = 91.18°$. Fe_2N-like silica has been reported previously from shock experiments on quartz (Sekine et al. 1987). However, in the present case the small amount of material and the spotty pattern do not allow us to decide clearly whether these peaks belong to Fe_2N-type silica. A broad diffraction feature at a Q-value slightly below the (011) reflection of the transitory silica phase may belong to disordered material related to this phase (see Fig. 2).

One month after this experiment, we collected diffraction patterns on the same sample at the same synchrotron beamline using identical methods. We found that the diffraction signal had broadened markedly. Extended irradiation with X-rays of 30 keV energy had no effect on the crystallinity. Thus, the previously observed change in crystallinity and crystal orientation during subsequent irradiation of the retrieved sample was not an effect of irradiation but of release of internal strain after recovery from the diamond cell chamber. This additional diffraction experiment also shows that defect-rich stishovite decays much faster than well-crystallized material. This finding is in good accordance with results from recent molecular dynamics simulations (Luo et al. 2006).

DISCUSSION

We suggest that our result shows that amorphous silica retrieved from shock experiments to about 57 GPa and 2100 K is the result of post-shock amorphization rather than amorphous material in the shock state. Formation of stishovite at 13 GPa, 300 K implies a very low kinetic barrier between this particular amorphous material and the crystalline state. In general, it is not possible to transform other polymorphs of silica or vitreous silica into stishovite- or $CaCl_2$-type silica at 300 K, at least not below ~100 GPa (Haines et al. 2001; Prakapenka et al. 2004). Furthermore, it requires pressures four times higher than observed here to obtain room-temperature transformation of low-pressure silica polymorphs into disordered phases characterized by sixfold to ninefold irregular coordination of Si by O (Haines et al. 2001; Kingma et al. 1996).

The other important point is the extreme coherence-length of the resultant crystalline phase, which is on the order of 10 μm of itinerant lattice periodicity without intersecting grain boundaries. Glasses have medium-range order. A glass-to-solid transition without subsequent collective recrystallization results in a fine-grained aggregate of untextured crystallites. This can be seen, for example, in samples quenched rapidly from the molten state. In the present case, we find a few large crystallites that result from the amorphous-to-solid transition although temperature is clearly too low to allow for collective recrystallization on the experimental time scale of minutes. The observed transition therefore cannot be a glass-to-solid transition. It resembles an order-disorder type transition where the length of lattice periodicity scales with the order parameter coherence length. The development from an initially small (<100 nm) lattice periodicity of an X-ray amorphous material into a very long (10 μm) periodicity of a coarse-grained aggregate of a few crystals resembles a Landau-type transition behavior.

The distinct behavior of the shock-recovered amorphous material, able to undergo an amorphous-to-solid transition at 300 K and moderate pressure, indicates that the amorphous material should be described as the result of slight, static, random displacements of atoms from their regular positions in the stishovite lattice as opposed to a material with medium-range order such as glass. The shock-retrieved amorphous silica therefore resembles metamict solids rather than vitreous materials. We note that the compression behavior of this material is complementary in an interesting way to that of quartz: crystalline quartz starts to undergo structural disorder and to amorphize above 15 GPa, 300 K under slow compression and non-hydrostatic conditions (Hemley et al. 1988; Hazen et al. 1989), whereas the present material is disordered at ambient conditions and recovers crystalline order at 13 GPa, 300 K. In both cases, the amorphous state is quenchable.

The amorphous-to-crystal transition at 13 GPa, 300 K also implies that, at this pressure and temperature, regular sixfold coordination of silica is energetically favorable over any of the structural deviations occurring in the amorphous state. If fourfold- or fivefold-coordinated structures were favorable, the material would continue to lose structural coherence while shifting further away from the rutile-type structure toward such phases. This is not what we observe. Thus, rutile-type silica represents at least a local energy minimum at 13 GPa, 300 K.

The high coherence of structural order as expressed in the formation of large crystallites upon recovery of full structural order suggests that the sample was coarse-grained or perhaps a single-crystal during shock. This inference also is consistent with the observed optical anisotropy that can be interpreted based on our present results as remnant intrinsic anisotropy of this slightly disordered material rather than the effect of residual stress. This high coherence length of structural order of stishovite contrasts with the partially powdery character of the coexisting transitory silica phase and suggests different conditions of formation during shock. If the bulk of the material is coarse-grained stishovite, the coexisting transitory phase could reside along grain boundaries of the stishovite crystallites that formed upon release. Thus, generation of the transitory phase can perhaps be assigned to frictional heating upon release due to shock-impedance mismatch between differently oriented stishovite grains, locally non-hydrostatic stresses, and weakened material strength at the grain boundaries during that part of the release path where the particle velocity is still high but stresses begin to drop below the yield strength of stishovite. Under shock, the stresses are approximating hydrostatic conditions if the shock stress is sufficiently above the Hugoniot elastic limit.

An alternative interpretation of the amorphous-to-solid transi-

tion in diaplectic amorphous silica is the concept of a ferroelastic glass recently proposed for amorphisation of silica induced by high static stress fields (Tolédano and Machon 2005). In this model, the amorphous state represents an array of ferroelastic domains too small to yield crystalline Bragg scattering. Exposure to high pressure and directed stress allows for re-orientation and for collective growth of such an array into large domains. This concept requires existence of intermediate low-symmetric structures in advance of stishovite recovery. It is possible that the monoclinic transitory silica phase (Luo et al. 2004) observed in our experiment plays this role. However, this phase is not ferroelastic but topologically disordered, which requires a modification of the mechanism proposed by Tolédano and Machon (2005). Also, this low-symmetry phase appears to form along with stishovite rather than in advance.

The formation of stishovite occupying most of the bulk of the sample in large grains strongly supports prograde formation of stishovite (or a closely related crystalline phase) from quartz by a solid-solid phase transition rather than local processes such as shear-heating (Tan and Ahrens 1990). In the latter case, one would expect lower yield and a fine-grained product. Furthermore, although the multiple shock path in our recovery chamber is somewhat different from a single shock, our findings suggest that stishovite may be recovered from amorphous silica which had been shocked to between ~15 and 38 GPa along the principal Hugoniot of quartz (Luo et al. 2003). The previous recovery of minor amounts of stishovite from experiments along the principal Hugoniot of quartz and fused silica therefore represent locally different release paths rather than inhomogeneities during shock.

Concluding remarks

Our results show that amorphous silica retrieved from shock experiments on quartz to peak pressures of 57 GPa, within the stishovite- and $CaCl_2$-type stability field, transforms into crystalline stishovite at ambient conditions during and after static recompression to 13 GPa, 300 K. No heating is necessary for this process. The amorphous-to-crystal transition is characterized by a long coherence length, resulting in formation of large crystallites. Therefore, the shock-recovered amorphous material studied here is a slightly disordered sixfold-coordinated silica phase but not a glass, which possesses only medium-range order. It is therefore most likely that stishovite (or a structurally closely related solid phase) re-presents the state this material had assumed during shock, while post-shock heating to 500–1000 K (Wackerle 1962; Boslough 1988; Luo et al. 2003) induced the observed slight disorder. This phenomenon of a probable memory-effect allows for physically more precise characterization of diaplectic silica "glass" and may be extended to other diaplectic "glasses" (amorphous materials recovered from shock to pressures and temperatures below the melting curve), and it adds support to the inferred solid-solid transformation mechanisms of bulk quartz into stishovite upon shock rather than to the alternative of local processes such as shear heating (Grady 1980), which would generate only small amounts of stishovite in an otherwise amorphous matrix.

Acknowledgments

This work was supported under the NNSA Cooperative Agreement DE-FC88-01NV14049 and under NASA PGG Grant NNG04G107G and Contribution no. 9144, Division of Geological and Planetary Sciences, California Institute of Technology. We thank V. Prakapenka, T. Sharp, and R. Jones for their very helpful comments. We thank M. Long and P. Gelle for support in performing the shock experiment and M. Somayazulu for assistance in the synchrotron diffraction experiment. Use of the HPCAT facility was supported by DOE-BES, DOE-NNSA, NSF, DOD-TACOM, and the W.M. Keck Foundation. APS is supported by DOE-BES under contract no. W-31-109-Eng-38.

References cited

Boslough, M.B. (1988) Postshock temperatures in silica. Journal of Geophysical Research, 93, 6477–9484.

Chao, E.C.T. (1967) Shock effects in certain rock-forming minerals. Science, 156, 192–203.

Chao, E.C.T. and Shoemaker, E.P. (1960) First natural occurence of coesite. Science, 132, 220–222.

DeCarli, P.S. and Milton, D.J. (1965) Stishovite: Synthesis by shock wave. Science, 147, 144–145.

Dera, P., Prewitt, C.T., Boctor, N.Z., and Hemley, R.J. (2002) Characterization of a high-pressure phase of silica from the Martian meteorite Shergotty. American Mineralogist, 87, 1018–1023.

El Goresy, A., Dubrovinsky, L., Sharp, T.G., Saxena, S.K., and Chen, M. (2000) A monoclinic post-stishovite polymorph of silica in the Shergotty meteorite. Science, 288, 1632–1634.

Ewing, R.C. (1999) Nuclear waste forms for actinides. Proceedings of the National Academy of Science U.S.A., 96, 3432–3439

Fiske, P.S., Nellis, W.J., Xu, Z., and Stebbins, J.F. (1998) Shocked quartz: A Si-29 magic-angle-spinning nuclear resonance study. American Mineralogist, 83, 1285–1292.

Grady, D.E. (1980) Shock deformation of brittle solids. Journal of Geophysical Research, 85, 913–914.

Gratz, A.J., Nellis, W.J., Christie, J.M., Brocious, W., Swegle, J., and Cordier, P. (1992) Shock metamorphism of quartz with initial temperatures—170 to 1000 °C. Physics and Chemistry of Minerals, 19, 267–288.

Haines, J., Léger, J.M., Gorelli, F., and Hanfland, M. (2001) Crystalline post-quartz phase in silica at high pressure. Physical Review Letters, 87, 155503-1–155503-4.

Hammersley, A.P., Svensson, S.O., Hanfland, M., Fitch, A.N., and Hausermann, D. (1996) Two-dimensional detector software: From real detector to idealised image or two-theta scan. High Pressure Research, 14, 235–248.

Hazen, R.M., Finger, L.W., Hemley, R.J., and Mao, H.K. (1989) High-pressure crystal-chemistry and amorphization of alpha-quartz. Solid State Communications, 72, 507–511.

Hemley, R.J., Jephcoat, A.P., Mao, H.K., Ming, M.C., and Maghnani, M.H. (1988) Pressure-induced amorphization of crystalline silica. Nature, 334, 52–54.

Kieffer, S.W., Phakey, P.P., and Christie, J.M. (1976) Shock processes in porous quartzite—transmission electron microscope observations and theory. Contributions to Mineralogy and Petrology, 59, 41–93.

Kingma, K.J., Mao, H.K., and Hemley, R.J. (1996) Synchrotron X-ray diffraction of SiO_2 to multimegabar pressures. High Pressure Research, 14, 363–374.

Kirfel, A., Krane, H.G., Blaha, P., Schwartz, K., and Lippmann, P. (2001) Electron-density distribution in stishovite, SiO_2: a new high-energy synchrotron-radiation study. Acta Crystallographica, A57, 663–677.

Kleeman, J.D. and Ahrens, T.J. (1973) Shock-induced transition of quartz to stishovite. Journal of Geophysical Research, 78, 5954–5960.

Langenhorst, F., Deutsch, A., Stöffler, D., and Hornemann, U. (1992) Effect of temperature on shock metamorphism of single-crystal quartz. Nature, 356, 507–509.

Langenhorst, F., Poirier, J.P., Deutsch, A., and Hornemann, U. (2002) Experimental approach to generate shock veins in single crystal olivine by shear melting. Meteoritics and Planetary Science, 37, 1541–1553.

Liu, L.G., Bassett, W.A., and Sharry, J. (1978) New high-pressure modifications of GeO_2 and SiO_2. Journal of Geophysical Research, 83, 2301–2305.

Luo, S.N., Ahrens, T.J., and Asimow, P.A. (2003) Polymorphism, superheating, and amorphization of silica upon shock wave loading and release. Journal of Geophysical Research, 108, 2421–2434.

Luo, S.N., Tschauner, O., Asimow, P.A., and Ahrens, T.J. (2004) A new dense silica phase: a possible connection between tetrahedrally and octahedrally coordinated silica. American Mineralogist, 89, 455–461.

Luo, S.-N., Zheng, L.Q., Tschauner, O. (2006) Solid-state disordering and melting of silica stishovite: the role of defects. Journal of Physics: Condensed Matter, 18, 659–668.

Murakami, M., Hirose, K., Ono, S., and Ohishi, Y. (2003) Stability of $CaCl_2$-type and BOX-PbO_2-type SiO_2 at high pressure and temperature determined by in-situ X-ray measurements. Geophysical Research Letters, 30, 1207–1210.

Ono, S., Hirose, K., Murakami, M., and Ishiki, M. (2002) Post-stishovite phase boundary in SiO_2 determined by in situ X-ray observations. Earth and Planetary Science Letters, 197, 187–192.

Prakapenka, V.P., Shen, G.Y., Dubrovinsky, L.S., Rivers, M.L., and Sutton, S.R. (2004) High-pressure induced phase transformation of SiO_2 and GeO_2: Difference and similarity. Journal of Physics and Chemistry of Solids, 65, 1537–1545.

Sekine, T., Akaishi, M., and Setaka, N. (1987) Fe_2N-type SiL_2 from shocked quartz. Geochimica et Cosmochimica Acta, 51, 379–381.

Sharma, S.M. and Sikka, S.K. (1996) Pressure-induced amorphization of materials. Progresses in Material Science, 40, 1–77.

Sharp, T.G., El Goersy, A., Wopenka, B., and Chen, M. (1999) A post-stishovite SiO_2 polymorph in the meteorite Shergotty: Implications for impact events. Science, 284, 1511–1513.

Shoemaker, E.P. and Chao, E.C.T. (1961) New Evidence for impact origin of Ries basin, Bavaria, Germany. Journal of Geophysical Research, 66, 3371–3378.

Stöffler, D. (1971) Progressive metamorphism and classification of shocked and brecciated crystalline rocks at impact craters. Journal of Geophysical Research, 76, 5541–5551.

Stöffler, D., Keil, K., and Scott, E.R.D. (1991) Shock metamorphism of ordinary chondrites. Geochimica et Cosmochimica Acta, 55, 3845–3867.

Tan, H. and Ahrens, T.J. (1990) Shock-induced polymorphic transitions in quartz, carbon, and boron-nitride. Journal of Applied Physics, 67, 217–224.

Tolédano, P. and Machon, D. (2005) Structural mechanism leading to a ferroelastic glass state: Interpretation of amorphization under pressure. Physical Review B, 71, 024210–024220.

Tschauner, O., Luo, S.N., Asimow, P.D., Ahrens, T.J., Swift, D.C., Tierney, T.E., Paisley, D.L., and Chipera, S.J. (2004) Shock-synthesized glassy and solid silica intermediate between four- and sixfold coordination. High Pressure Research, 24, 471–479.

Tschauner, O., Willis, M.J., Asimow, P.D., and Ahrens, T.J. (2005) Effective liquid metal-silicate mixing upon shock by power-law droplet size scaling in Richtmyer-Meshkov like perturbations. LPI Contributions, 1234, 1802.

Wackerle, J. (1962) Shock-wave compression of quartz. Journal of Applied Physics, 33, 922–937.

MANUSCRIPT RECEIVED JUNE 20, 2005
MANUSCRIPT ACCEPTED MAY 30, 2006
MANUSCRIPT HANDLED BY RHIAN JONES